2024-10-02

Exergy analysis and performance testing of a gravitational water vortex turbine runner for small hydropower plants: An Experimental Approach

Faraji, Adam

AJOL

https://doi.org/10.4314/tjs.v50i3.13

Tanzania Journal of Science 50(3): 580-590, 2024
ISSN 0856-1761, e-ISSN 2507-7961

Exergy analysis and performance testing of a gravitational water vortex turbine runner for small hydropower plants: An Experimental Approach

Adam Faraji[1,2], Yusufu Abeid Chande Jande[1,3] Thomas Kivevele[1,3]

[1]School of Materials, Water and Environmental Sciences (MEWES), The Nelson Mandela African Institution of Science and Technology, Nelson Mandela Rd, P.O BOX 447, Arusha, Tanzania

[2]Department of Mechanical Engineering, Arusha Technical College, Junction of Moshi-Arusha and Nairobi Road, P. O. BOX 296, Arusha, Tanzania

*[3]Water Infrastructure and Sustainable Energy Futures Center, The Nelson Mandela African Institution of Science and Technology, Nelson Mandela Rd, P.O BOX 9124 Nelson Mandela, Arusha, Tanzania. *Corresponding Author; Adam Faraji, 0763 868 540, farajia@nm-aist.ac.tz*

Received 30 April 2024, Revised 8 July 2024, Accepted 19 July, Publ. 30 Sept. 2024

https://dx.doi.org/10.4314/tjs.v50i3.13

Abstract

Gravitational water vortex power plants (GWVPPs) have recently gained popularity due to their low initial investment, simple design, ease of maintenance, and low head utilization. However, the technology suffers from poor performance issues caused by the non-optimized parameters of its crucial components, such as the runner. In this study, the performance of a runner (16° blade-hub angle, six blades, and a curved blade profile) for a GWVPP was experimentally examined. The study also employed an exergy analysis. The experimental results revealed that the efficiency of the GWVPP system was in the range of 9.84% to 25.35%, the torque was in the range of 0.08 to 0.23 Nm, and the output power was in the range of 2.96 to 7.33 W. Furthermore, an exergy analysis of the system showed an exergy efficiency of 43.58%. Additionally, the error analysis of the GWVPP revealed ranges of 0.1 - 0.5 W for power, 0.01 - 0.03 Nm for torque, and 1.3–3.1% for efficiency, suggesting that the experimental setup and instrumentation of this study were reasonably accurate. Based on the results, the new vortex runner and GWVPP system are recommended for energy generation in low-head, low-flow small hydropower plants.

Keywords – Micro-hydropower; gravitational water vortex; runner; exergy efficiency; test rig.

Introduction

The overreliance on traditional energy sources, like fossil fuels, has led to environmental concerns, prompting the development of renewable energy options like hydro-turbine power generation, which is cost-effective and practical (Okot 2013). Hydropower (HP) projects are classified based on size, either small (SHP) or large (LHP), but this classification varies by country due to a lack of consensus (Paish 2002). Pico, micro, mini, and small systems are subcategories of SHP, with pico generating less than 10 kW, micro generating over 10 kW but less than 100 kW, mini generating over 100 kW but less than 1 MW (Kaunda et al. 2012, Timilsina et al. 2018). SHP systems, either reservoirs or run-of-river types, generate power by diverting water from a river's main channel through a weir, reducing investment costs. The system's working principle involves converting falling water energy into rotating shaft power through a turbine, which can be impulse or reaction-based (Paish 2002).

In recent years, Micro-hydropower systems are gaining popularity as a renewable energy technology to provide electricity to remote areas with high costs and low incomes (Williamson et al. 2014). The selection of a

turbine for a hydroelectric power plant (HPP) site is influenced by factors such as available head and flow rate, generator operating speed, and power requirements for low flow conditions (Okot 2013). Micro-HP turbines like Archimedes screw turbine, gravitational water vortex power plant (GWVPP), and waterwheel turbine are suitable for low head and low flow rate conditions.

GWVPP is a micro-HP scheme suitable for low flow rates and heads in rivers and streams, offering a new addition to the 0.7 to 2 m head range (Zotlöterer 2017). The GWVPP system, consisting of a runner, basin, and canal, offers environmental safety, ease of manufacture, low maintenance costs, no water storage, increased surface water area, and aquatic life safety (Dhakal et al. 2014, Rahman et al. 2017 and Khan et al. 2018).

Recent interest in GWVPPs has led to studies assessing their performance, focusing on energy efficiency. The impact of runners' shapes on overall efficiency has been studied. Dhakal's study found that curved blades were 82% more efficient than twisted and straight blades, outperforming both profiles (Dhakal et al. 2017b). Kueh's experimental study on runner profiles revealed that despite a 22.24% improvement in efficiency, the ideal efficiency was not achieved due to limitations in friction torque and load-cell components (Kueh et al. 2017). Chen's study on basin-to-blade ratio setups revealed that cross-flow blades outperformed other runner profiles with an efficiency of 68.84% (Khan et al. 2018). Two different runner profiles were optimized numerically, with the findings indicating that curved profiles exhibited better efficiency (ranging from 9.80% to 25.89%) compared to flat profiles (with efficiency ranging from 8.8% to 23.32%) (Faraji et al. 2022).

Previous research on GWVPPs was primarily relied on traditional energy efficiency, but exergy efficiency offers a more comprehensive view of energy quality. Exergy efficiency measures the valuable work a system can produce, considering irreversible processes and inefficiencies. This study applied an exergy-based method to evaluate the effectiveness of a GWVPP, aiming to experimentally study the GWVPP system by using the optimized parameters of the numerical study of Faraji et al. (2022) and perform an exergy analysis of the GWVPP system. The study involved the complete design, manufacturing, and experimental testing of a GWVPP test rig. The test rig underwent evaluation at different rotational speeds, assessing power, torque, and efficiency and applying the first law of thermodynamics to determine system exergy efficiency.

Materials and Methods

Experimental set-up

The experimental test rig includes a 1000 L water storage tank, a two hp centrifugal pump, a 1000 L overhead reservoir, a GWVPP basin, a canal, and a runner assembly. The basin and canal are placed above the water storage tank, and the GWVPP runner optimizes the design with specific parameters. These parameters were selected based on a previous study by Faraji et al. (2022). The GWVPP runner's performance was evaluated using digital tachometers and Prony brake dynamometers at various operating speeds. The experimental test rig (Figure 1) was located at the Nelson Mandela African Institution of Science and Technology (NM-AIST) in Tanzania. Replicas or controls were used for reliability and statistical significance.

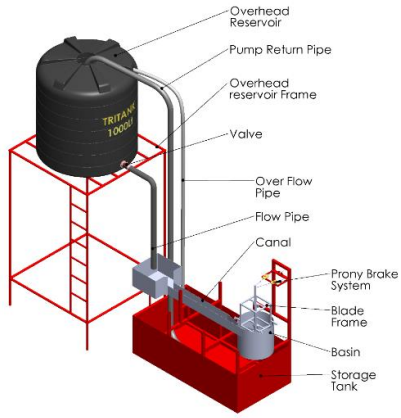

Figure 1: Experimental setup of the three-dimensional gravitational water vortex power plant (GWVPP).

The experimental setup consisted of a blade frame/support, overhead reservoir frame, pump, pipe, storage tank, and overhead reservoir. The blades were secured with mild steel sheets and angle iron, while the overhead reservoir was made from class B black steel pipe. A 2 hp centrifugal pump supplied water to the overhead reservoir, and a 50 mm diameter flexible pipe supplied water to the basin inlet. A storage tank was installed to prevent wastage, and an overhead reservoir was used to create an artificial flow to the canal, storing water that eventually flowed to the canal entrance. The water is pumped to the reservoir, guided by gravity, and a ball gate valve regulates the flow rate.

Selection of materials

The experimental test rig, primarily made of steel, was constructed for its mobility, portability, and cost-effectiveness, as detailed in Table 1, showcasing the local materials used.

Table 1: The experimental test rig: materials, specifications, and quantity.

Part	Materials	Specifications	Quantity
Basin	Mild steel sheet	1570 × 500 × 2 mm	1 pc*
Canal	Mild steel sheet	2100 × 400 × 2 mm	1 pc
Runner	Mild steel sheet	300 × 180 × 2 mm	6 pcs
	Black pipe	Φ50 × 300 mm	1 pc
Storage tank	Mild steel sheet	2000 × 600 × 2 mm	2 pcs
	Mild steel sheet	1000 × 600 × 2 mm	2 pcs
	Mild steel sheet	2000 × 1000 × 2 mm	1 pc
	Angle iron	40 × 40 × 3 mm	2 pcs
Runner support	Square hollow section	20 × 20 × 1.5 mm	2 pcs
	Angle Iron	40 × 40 × 3 mm	1 pc
	Mild steel shaft	Φ40 × 1200 mm	1 pc
	Bearing	CFK P206	2 pcs
Prony brake	Square hollow section	20 × 20 × 1.5 mm	1 pc
	Wire rope	Φ8 × 800 mm	1 pc
	Bolt and nut	M12 v 150 mm	1 pc
	Iron block	12 × 12 × 300 mm	1 pc
Overhead reservoir	Black pipe (class B)	Φ100 × 2500 mm	6 pcs
Frame	Square hollow section	40 × 40 × 2 mm	4 pcs

* pc – piece

Basin and canal fabrication

The basin and canal structures were made from mild steel iron sheets, with the inlet width adjusted according to the optimized design, as shown in production drawings and Figure 2.

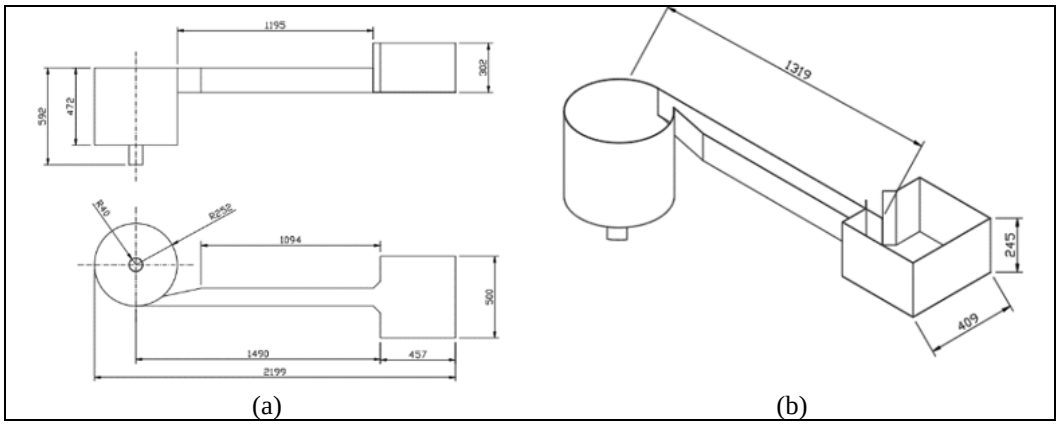

Figure 2: Basin and canal: (a) orthographic view, (b) isometric view. All dimensions are in millimeters.

Runner fabrication

Experimental work used a six-blade curved-blade profile type runner made from 1 mm mild steel sheets to reduce costs and ensure easy shape acquisition, as shown in Figure 3.

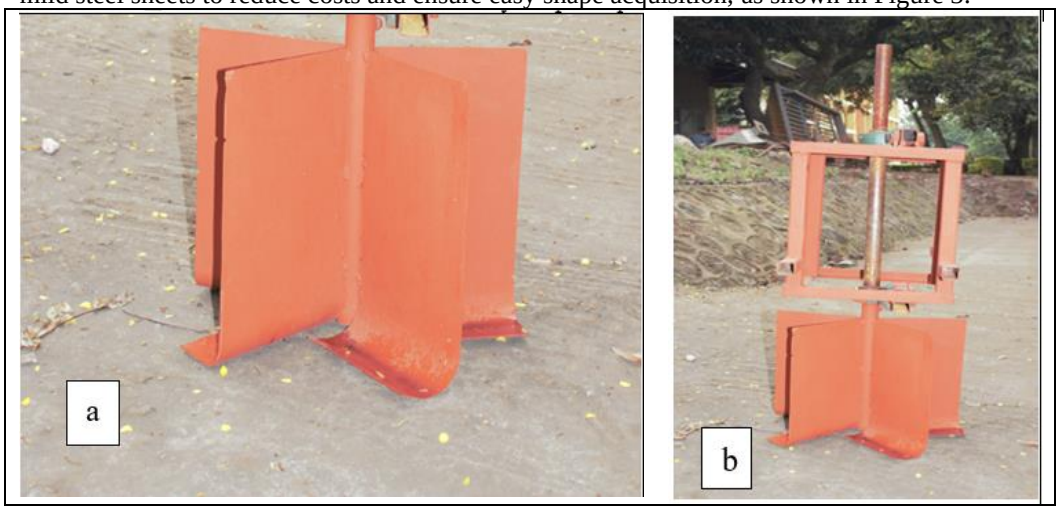

Figure 3 Fabricated blades used in the experimental setup: (a) blades and (b) blades with shaft support.

Data collection procedure

The experiments used the bucket or volumetric method to measure the flow rate by closing the basin aperture and opening the overhead reservoir valve, a method similar to previous studies (Gheorghe-Marius and Tudor 2013, Marian et al. 2013, Nishi and Inagaki 2017). Equation (1) was used to determine the flow rate, Q, for the existing system.

$$Q = \frac{Volume\ of\ the\ basin}{Time\ spent\ to\ fill\ the\ basin} \quad (1)$$

The upper frame of a vortex air core runner was supported using a class B black

steel tube to support the shaft and bearings. Data was collected by determining the system's torque and rotation speed using Mulligan and Hull (2010) and Dhakal et al. (2017) methods. A Prony braking mechanism was used to measure brake force and torque. A braking system was installed to measure output power and friction torques. The runner's rotational speed was measured using a digital tachometer. Data collection began with the runner at rest and continued with the turbine's rotational speed. The output power, torque, and efficiency were determined using equations (2), (3), and (4), respectively which are according to Mulligan and Hull (2010) and (Dhakal et al. (2017a).

$$P_{output} = \frac{2\pi grN}{60}\left(M_{weight} - M_{counterweight}\right) \quad (2)$$

where, r is the radius of the pulley, M_{weight} is the mass of the first weigh scale, and $M_{counterweight}$ is the mass of the second weigh scale.

$$T = gr\Delta m \quad (3)$$

where, g, is the acceleration due to gravity, r is the pulley radius, and Δm is the change in mass between the first and second weigh scales.

$$H = \frac{T\omega}{\rho QgH} \quad (4)$$

where, ω is the rotational speed in rpm and H is the head.

Exergy analysis of the system

The first law of thermodynamics was applied to analyze the exergy of a system, considering the control volume as an open system, and using Equation (5) (Abuelnuor et al. 2020).

$$0 = \sum\left(1 - \frac{T_o}{T_j}\right)\dot{Q} - W + \sum_i m_i e_{fi} - \sum_e m_e e_{fe} - E_d \quad (5)$$

where T_j = temperature at the boundary (K), T_o = temperature at the environment (K), W = energy transfer via control volume (W), $\dot{m}$ = mass flow rate (kg/s), Q = heat transfer rate (W). Furthermore, $e_f = h - h_o - T_o(s - s_o) + 0.5(V^2) + gz$; where h_o = enthalpy (kJ / kg), h = enthalpy of the working fluid (kJ / kg), V = velocity of the working fluid (m/s), g = acceleration gravity (m^2/s), s = entropy of the working fluid (kJ/kg K), s_o = environment entropy (kJ / kg K), E_d = destruction of exergy due to irreversibility (W) and z = elevation (m).

The control volume operated under ambient conditions, which were assumed to be 25 ° C (temperature), 1 atm (atmospheric pressure), and 1000 kg/m^3 (density of water). These assumptions reduced Equation (5) to Equation (6), which was used to calculate E_d (exergy destruction due to irreversibility).

$$E_d = \dot{m}\left[\left(\frac{c_1^2 - c_2^2}{2}\right) + g(z_1 - z_2)\right] - W \quad (6)$$

where c_1 and c_2 are the water velocities in m/s at the inlet and outlet, respectively. The water velocities were determined by the division of flow by the respective inlet and outlet areas and z_1 and z_2 were the elevations in m at the input and outlet, respectively. Elevations were determined using a tape measure, as shown in Figure 4.

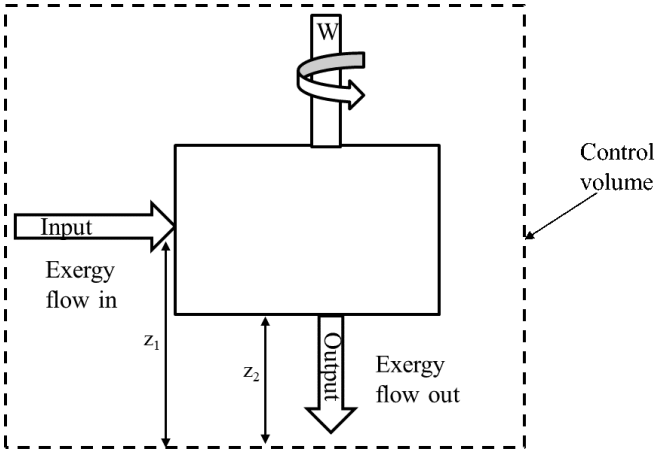

Figure 4: Schematic of exergy flow under the controlled volume of GWVPP system.

The steady-flow energy equation (SFEE) was utilized to calculate the work done by the system, considering the conservation of energy Equation 7 (Dixon and Hall 2013) was used to determine the work done (W) by the system.
The energy balance was as follows:

Energy input = Energy output

$$\dot{m}\left(h_1 + \frac{c_1^2}{2} + z_1 g\right) + Q = \dot{m}\left(h_2 + \frac{c_2^2}{2} + z_2 g\right) + W \quad (7($$

where h_1 and h_2 are the specific enthalpies at the inlet and outlet, respectively, $\frac{1}{2}c^2$ is the kinetic energy per unit mass, gz is the potential energy per unit of mass, and W is work (W).
A hydraulic turbine operates with no heat transfer, work W = +W work produced, and no change in internal energy, $u_1 = u_2$

Thus, $h_1 - h_2 = u_1 + p_1 v_1 - (u_2 + p_2 v_2)$

$h_1 - h_2 = p_1 v_1 - p_2 v_2)$
Equation (7) becomes:

$$W = \dot{m}\left(\frac{c_1^2 - c_2^2}{2} + g(z_1 - z_2) + p_1(v_1 - v_2)\right) \quad (8)$$

The study calculates the specific volume of a fluid by comparing the atmospheric pressure (p_1) and specific volumes v_1 and v_2 at the inlet and outlet.
The exergy efficiency of the system was determined by Equation (9):

Thus, the exergy efficiency $= \frac{Exergy\ output}{Exergy\ input}$ which is according to Vakilabadi et al. (2019), Abuelnuor et al. (2020) and Moshi (2021).

$$\varphi = \frac{W}{W + E_d} \quad (9)$$

Error analysis

An error analysis was conducted to identify and quantify errors in experimental measurements, identifying potential sources such as speed recording tachometers and weigh scales, to capture random uncertainty (Bachynski et al. 2019). To calculate the random uncertainty, S_R, of the experimental data, the following equation was used:

$$S_R = \frac{S_x}{\sqrt{N-1}} \quad (10)$$

where S_x is the standard deviation of both speed and mass.

The study assessed the impact of errors on power, torque, and efficiency parameters in tachometer and weigh scale measurements using propagating errors, utilizing equations for power, torque, and efficiency (Figliola and Beasley 2020).

$$\delta P = P\sqrt{\left(\frac{\delta\omega}{\omega}\right)^2 + \left(\frac{\delta\Delta m}{\Delta m}\right)^2} \quad (11)$$

$$\delta T = \delta\Delta m \quad (12)$$

$$\delta\eta = \eta\sqrt{\left(\frac{\delta T}{T}\right)^2 + \left(\frac{\delta\omega}{\omega}\right)^2} \quad (13)$$

Results and Discussions

Performance analysis of the GWVPP runner

The performance analysis of the GWVPP runner revealed an output power range of 2.96-7.33 W, torque of 0.08-0.23 Nm, and efficiency of 9.84%-25.35%. The higher efficiency was attributed by the optimized working parameters. The experimental efficiency was slightly lower than the numerical analysis of which was reported a maximum efficiency of 25.89% (Faraji et al. 2022). Figures 5 - 7 displays the performance curves showing maximum power (7.63 W) and torque (0.231 Nm) at a speed of 2.64 rad/s, with the highest efficiency (25.35%), indicating stable vortex flow without distortion (Dhakal et al. 2017 and Khan et al. 2018). The experiment exhibited excellent performance due to stable vortex flow and uniform water flow, resulting in maximum power, torque, and efficiency. Reduced rotational speed affected performance due to distorted vortex and basin water level changes. The optimal speed was 2.64 rad/s, ensuring maximum performance. The study found that the runner's rotational speed significantly influenced output power, torque, and efficiency. A zero-output power, torque, and efficiency value corresponded to the maximum rotational speed without braking force. When load was applied, rotational speed decreased, suggesting increased braking force and undistorted vortex flow as supported by Khan et al. (2018), Dhakal et al. (2017) and Kueh et al. (2017).

The performance parameters decreased due to a distorted vortex caused by disturbance in vortex flow and changes in basin water level, resulting from a further reduction in rotational speed (Khan et al. 2018, Kueh et al. 2017). The performance parameters and rotational speed in turbines have an inverse relationship until a maximum value is reached, this is according to studies by Khan et al. (2018), Ullah et al. (2019) and Saleem et al. (2020). The highest efficiency is achieved when the runner's rotation speed is half the vortex speed, as the vortex flow generates lift and rotation. Slow or fast rotation can reduce turbine efficiency (Mulligan and Casserly 2010 and Rahman et al. 2016). The vortex flow created a pressure gradient along the turbine blades, which caused them to generate lift and rotate (Li et al. 2023). The study analysis provides valuable insights into the design and operation of micro-HP systems, enabling engineers to optimize efficiency and performance by adjusting input parameters.

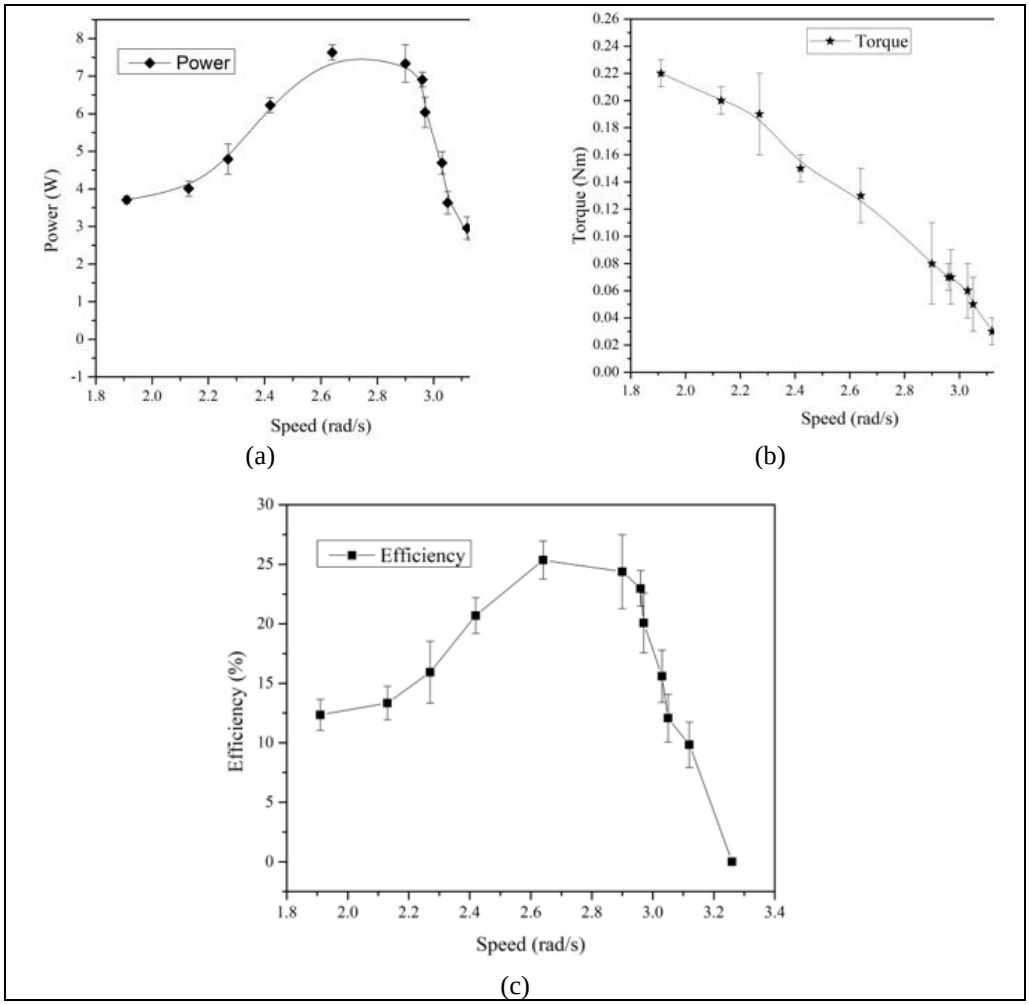

Figure 5: Effect of rotation speed on (a) runner power (b) runner torque (c) runner efficiency.

Exergy analysis

The study found a high exergy efficiency of 43.58% for the GWVPP runner, slightly higher than previous studies, such as Hossain et al. (2020) ranging from 35.0% to 39.2% and Maruf et al. (2021) ranging from 35.07% to 36.59%. This efficiency is attributed to optimized working parameters, such as speed, blade-hub angle, number of blades, and blade profile. Exergy efficiency measures the proportion of input energy converted into useful work (Rosen and Dincer 2001).

Error analysis

The study found that the power, torque, and efficiency measurements were reliable and precise, with error ranges ranging from 0.1 to 0.5 W, 0.01 to 0.03 Nm and 1.3 – 3.1%, respectively (Figures 5 - 7). The torque measurement process was more reliable and less prone to errors, possibly due to the propagation of errors in these parameters. Efficiency errors were generally low, with most falling within the 1.3% to 3.1% range. The efficiency error depended on both power and torque errors, with lower errors at lower rotational speeds and higher errors at higher speeds. Overall, the experimental setup and instrumentation were reasonably accurate.

Conclusion

The study evaluated the efficiency and capabilities of a gravitational water vortex power plant (GWVPP) turbine runner using

exergy analysis and performance testing methods. The results shows that the turbine runner efficiencies ranging from 9.84% to 25.35%, torque values ranging from 0.08 Nm to 0.23 Nm, and output power ranging from 2.96 to 7.33 W. From these results, it is clearly shown that GWVPP technology offers a low-cost alternative to traditional hydroelectric power plants, with minimal maintenance requirements and efficient utilization of low head resources. Moreover, beyond its immediate applications, this research contributes to the broader discourse on sustainable energy solutions. By demonstrating the feasibility and efficacy of GWVPP technology. Lastly, but not least, the studies from this research advocates for the exploration and adoption of innovative approaches to harnessing innovative water energy sources. So, in this case, future energy research should focus on optimizing GWVPP energy capacity, its scalability as well as environmental impact assessments.

Data Availability

Data supporting the findings of this study are available in the article.

Conflict of Interest

The authors declare that they have no conflict of interest.

Acknowledgment

We acknowledge the financial support of the Water Infrastructure and Sustainable Energy (WISE Futures) Centre of Excellence of the Nelson Mandela African Institution of Science and Technology.

References

Abuelnuor AA, Ahmed K, Saqr KM, Nogoud YA and Babiker ME 2020 Exergy analysis of large and impounded hydropower plants: Case study El Roseires Dam (280 MW). *Environmental Progress & Sustainable Energy,* 39**,** e13362.

Bachynski E, Thys M and Delhaye V 2019 Dynamic response of a monopile wind turbine in waves: Experimental uncertainty analysis for validation of numerical tools. *Applied Ocean Research,* 89**,** 96-114.

Dhakal R, Bajracharya T, Shakya S, Kumal B, Kathmandu N, Khanal K, Kavre N, Williamson S, Gautam S and Ghale D 2017 Computational and experimental investigation of runner for gravitational water vortex power plant. Proceedings of a meeting held, 2017a. 8.

Dhakal R, Bajracharya T, Shakya S, Kumal B, Khanal K, Williamson S, Gautam S and Ghale D 2017 Computational and experimental investigation of runner for gravitational water vortex power plant. 2017 IEEE 6th International Conference on Renewable Energy Research and Applications (ICRERA), 2017b San, Diego, USA. IEEE Publisher, 365-373.

Dhakal S, Nakarmi S, Pun P, Thapa AB and Bajracharya TR 2014 Development and testing of runner and conical basin for gravitational water vortex power plant. *Journal of the Institute of Engineering,* 10**,** 140-148.

Dixon SL and Hall C 2013 Fluid mechanics and thermodynamics of turbomachinery, Butterworth-Heinemann.

Faraji A, Jande YAC and Kivevele T 2022 Performance analysis of a runner for gravitational water vortex power plant. *Energy Science & Engineering,* 10**,** 1055-1066.

Figliola RS and Beasley DE 2020 Theory and design for mechanical measurements, John Wiley & Sons.

Gheorghe-Marius M and Tudor S 2013 Energy capture in the gravitational vortex water flow *Journal of Marine Technology & Environment,* 1.

Hossain S, Chowdhury H, Chowdhury T, Ahamed JU, Saidur R, Sait SM and Rosen MA 2020 Energy, exergy and sustainability analyses of Bangladesh's power generation sector. *Energy Reports,* 6**,** 868-878.

Kaunda CS, Kimambo CZ and Nielsen TK 2012 Potential of small-scale hydropower for electricity generation in Sub-Saharan Africa. *ISRN Renewable Energy,* 2012**,** 1-15.

Khan NH, Cheema TA, Chattha JA and Park CW 2018 Effective basin–blade configurations of a gravitational water

vortex turbine for microhydropower generation. *Journal of Energy Engineering,* 144**,** 04018042.

Kueh T, Beh S, Ooi Y and Rilling D 2017 Experimental study to the influences of rotational speed and blade shape on water vortex turbine performance. Fifteenth Asian congress of fluid mechanics (15ACFM), 2017 Sarawak, Malaysia. IOP Publishing 822 (2017) 012066, doi:10.1088/1742-6596/822/1/012066, .

Li W, Huang Y, Ji L, Ma L, Agarwal RK and Awais M 2023 Prediction model for energy conversion characteristics during transient processes in a mixed-flow pump. *Energy,* 271**,** 127082.

Marian MG, Sajin T and Azzouz A 2023 Study of micro hydropower plant operating in gravitational vortex flow mode. Applied Mechanics and Materials, 2013. Trans Tech Publ, 601-605.

Maruf MH, Rabbani M, Ashique RH, Islam MT, Nipun MK, Haq MAU, Al Mansur A and Shihavuddin A 2021 Exergy based evaluation of power plants for sustainability and economic performance identification. *Case Studies in Thermal Engineering,* 28**,** 101393.

Moshi R 2021 The Exergy Analysis for the Air Gasification in a Hybrid Fixed Bed Gasifier.

Mulligan S and Casserly J 2010 The hydraulic design and optimisation of a free water vortex for the purpose of power extraction. *Sligo: Institute of Technology Sligo*.

Mulligan S and Hull P 2010 Design and optimisation of a water vortex hydropower plant. *Sligeach: Department of Civil Engineering and Construction, IT Silgo*.

Nishi Y and Inagaki T 2017 Performance and flow field of a gravitation vortex type water turbine. *International Journal of Rotating Machinery,* 2017.

Okot DK 2013 Review of small hydropower technology. *Renewable and Sustainable Energy Reviews,* 26**,** 515-520.

Paish O 2002 Small hydro power: technology and current status. *Renewable and sustainable energy reviews,* 6: 537-556.

Rahman M, Hong TJ, Tang R, Sung LL and Tamiri FBM 2016 Experimental study the effects of water pressure and turbine blade lengths & numbers on the model free vortex power generation system. *International Journal of Current Trends in Engineering & Research (IJCTER),* 2**,** 13-17.

Rahman M, Tan J, Fadzlita M and Muzammil A 2017 A Review on the development of Gravitational Water Vortex Power Plant as alternative renewable energy resources. International Conference on Materials Technology and Energy, 2017. IOP Publishing, 217 (2017) 012007.

Rosen MA and Dincer I 2001 Exergy as the confluence of energy, environment and sustainable development. *Exergy, an International journal,* 1**,** 3-13.

Saleem AS, Cheema TA, Ullah R, Ahmad SM, Chattha JA, Akbar B and Park CW 2020 Parametric study of single-stage gravitational water vortex turbine with cylindrical basin. *Energy,* 200**,** 117464.

Timilsina AB, Mulligan S and Bajracharya TR 2018 Water vortex hydropower technology: a state-of-the-art review of developmental trends. *Clean Technologies and Environmental Policy,* 20**,** 1737-1760.

Ullah R, Cheema TA, Saleem AS, Ahmad SM, Chattha JA and Park CW 2019 Performance analysis of multi-stage gravitational water vortex turbine. *Energy Conversion and Management,* 198**,** 111788.

Vakilabadi MA, Bidi M, Najafi A and Ahmadi MH 2019 Exergy analysis of a hybrid solar-fossil fuel power plant. *Energy Science & Engineering,* 7**,** 146-161.

Williamson S, Stark B and Booker J 2014 Low head pico hydro turbine selection using a multi-criteria analysis. *Renewable Energy,* 61**,** 43-50.

Zotlöterer. 2017. *Gravitation water vortex power plants* [Online]. Available: http://www.zotloeterer.com/welcome/gravitation-water-vortex-power-plants/. Accessed on 2 May 2022 [Accessed].